Significantly Enhanced SAW Transmission in Voltage Tunable GaAs/$LiNbO_3$ Hybrid Devices

Markus Rotter[*+], Werner Ruile[*], Daniela Bernklau[*], Henning Riechert[*], and Achim Wixforth[+]

[*]Siemens AG, Corporate Technology, D-81730 München, Germany
[+]Sektion Physik der LMU and CeNS, Geschw.-Scholl-Platz. 1, D-80539 München, Germany

***Abstract* — Thin GaAs quantum well structures fused onto $LiNbO_3$ substrates using the epitaxial lift off technology offer the possibility to control the SAW velocity via field effect. The tunability of the conductivity in the Galliumarsenid quantum well results in a large change of the SAW velocity and phase. This effect is in general accompanied by an attenuation over a small region of conductivity, decreasing the device performance. We show that a lateral modulation of the in-plane conductivity distributes the SAW attenuation over the whole voltage tuning range. Employing this technique, the maximum attenuation of the hybrid SAW device is significantly reduced. Our approach opens new possibilities for voltage controlled SAW devices. Single-chip voltage controlled SAW oscillators, variable broadband delay lines and remote SAW voltage sensors can be realized.**

1. GaAs/$LiNbO_3$-HYBRIDS

The propagation velocity of surface acoustic waves (SAW) is strongly affected by the electrical boundary condition on the surface of the piezoelectric material. In conventional SAW devices the surface impedance is fixed by the design and usually can not be tuned externally. The combination of a piezoelectric material with the voltage tunable surface impedance of a semiconductor device, however, allows for continuously changing the velocity. A large change of SAW velocity can be achieved on a material with a large electromechanical coupling coefficient K^2, e.g. $LiNbO_3$. We demonstrated a quasi-monolithic combination of $LiNbO_3$ and a GaAs quantum well structure for controlling the SAW velocity[1,2].

This combination is achieved using the Epitaxial Lift-off technology (ELO) which was developed by Yablonovitch[3] et al.. Hohkawa et al. employed the process for the first time for SAW devices[4]. To fabricate the hybrids, a semiconductor layer system is grown by molecular beam epitaxy. On top of the GaAs substrate a AlAs sacrificial layer is grown, followed by a modulation doped InGaAs quantum well containing a two-dimensional electron system (2DES) (see Fig. 1). After covering the semiconductor structure, the AlAs layer is selectively etched in hydrofluoric acid. Then the active layer system containing the 2DES is removed from the substrate and transferred onto the $LiNbO_3$-chip (128° rot. YX-cut) with the SAW transducer structure. The ELO film is tightly fixed only by van der Waals forces. After this ELO process the semiconductor film, which has a thickness of 0.5 µm, is patterned as shown in Fig. 1. Typical values for carrier concentration and room temperature mobility are $N_s = 5\times10^{11}$ cm^{-2} and $\mu = 4000$ cm^2/Vs. Since the 2DES is very close to the $LiNbO_3$ surface, the conductivity of the electron system strongly influences the SAW propagation velocity v.

2. ATTENUATION AND VELOCITY CHANGE IN THE HYBRID

The interaction of the surface acoustic wave and the 2DES results in a change of SAW velocity v and an attenuation Γ of the transmitted SAW intensity $I = I_0 \exp(-\Gamma l)$, where l is the length of the ELO film in the direction of SAW propagation[5,6]. The effect of a thin semiconducting layer on surface acoustic waves was examined by Ingebrigsten. For our hybrid system, the sheet conductivity σ of the 2DES influences Γ and v as follows:

$$\Gamma = K_H^2 \frac{\pi}{\lambda} \frac{\sigma/\sigma_m}{1+(\sigma/\sigma_m)^2}$$
$$\frac{v - v_{sc}}{v_{oc}} = \frac{\Delta v}{v_{oc}} = K_H^2 \frac{1}{2} \frac{1}{1+(\sigma/\sigma_m)^2}, \quad (1)$$

where λ is the SAW wavelength in the hybrid, v_{sc} denotes the hybrid velocity for the highly conductive electron system and v_{oc} the hybrid velocity for a depleted electron system. K_H^2 is the effective hybrid coupling coefficient

to be presented at the IEEE Ultrasonics Symposium 1998 in Sendai, Japan

  0-7803-4095-7/98/$10.00

which is smaller than K^2 of $LiNbO_3$, because the gate electrode on top of the ELO-film causes the velocity for a depleted electron system to be smaller than the velocity for a free $LiNbO_3$ surface. For a frequency of $f = 340$ MHz and $f = 434$ MHz and the described layer structure, the hybrid coupling coefficient is $K_H^2 = 3.3\%$ and $K_H^2 = 3.8\%$, respectively[7]. The coefficient σ_m denotes the conductivity where maximum attenuation occurs and is for $f = 340$ MHz approximately given by $\sigma_m = v\varepsilon_0\left(\sqrt{\varepsilon_{11}^T\varepsilon_{33}^T - \varepsilon_{13}^T\varepsilon_{31}^T} + 1\right) = 2.1\times10^{-6}\Omega^{-1}$ with ε_{ii}^T being the dielectric constants of $LiNbO_3$ under constant stress conditions. If a field effect voltage is applied to the gate electrode, the quantum well is depleted, resulting in a reduction of the sheet conductivity σ. This leads to an increase of SAW velocity.

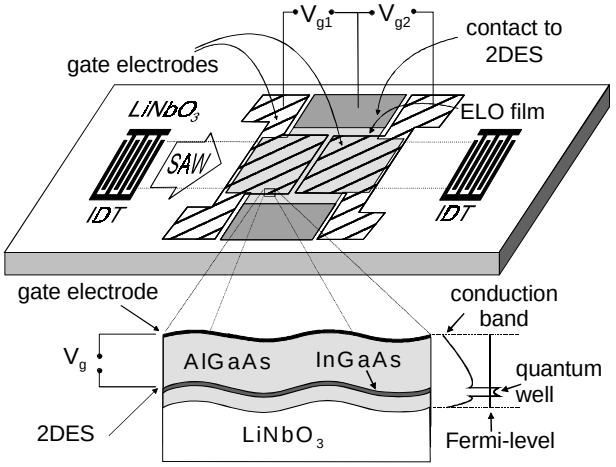

Fig. 1. Schematic sketch of the hybrid device with two gates on top of the ELO film. The thickness of the ELO film is 0.5 µm and the distance between $LiNbO_3$ and 2DES is just 32 nm.

If the gate voltage is applied homogeneously across the whole area of the ELO film, the change in SAW velocity is accompanied by a relatively large attenuation according to Eq. 1, which can be seen in Fig. 2 (see traces '$V_{g1} = V_{g2} = V_g$'). The insertion attenuation at $V_g = 0$ can be attributed to the bare SAW chip and the mechanical attenuation caused by the ELO film[7]. However, the attenuation maximum at $\sigma = \sigma_m$ limits device performance in the corresponding range of the gate bias. Therefore, we developed new device designs for the reduction of this attenuation. In principle, the idea is to distribute the attenuation over the whole range of gate bias, reducing the maximum attenuation at $\sigma = \sigma_m$. This can be achieved by dividing the ELO film into separated areas at different gate potentials. First, we discuss multiple gate structures, where different gate voltages are applied. Secondly, devices with a homogenous gradient of gate bias in direction of SAW propagation are presented.

3. Multiple Gate Structures

Fig. 1 shows the geometry of a hybrid device with two gate electrodes on top of the ELO film. The experimental results for this geometry are displayed in Fig. 2. If the gate voltage is applied to only one gate, with zero bias on the other, a phase shift and an attenuation of the transmitted RF signal can be seen (traces 'Gate 1' and 'Gate 2' in Fig. 2). Both gates show similar behavior. If the same gate voltage is applied to both gates at same time, attenuation and phase shift are added, resulting in a large phase shift and a nearly doubled attenuation at $V_g = -7.7$ V (see traces '$V_{g1} = V_{g2} = V_g$').

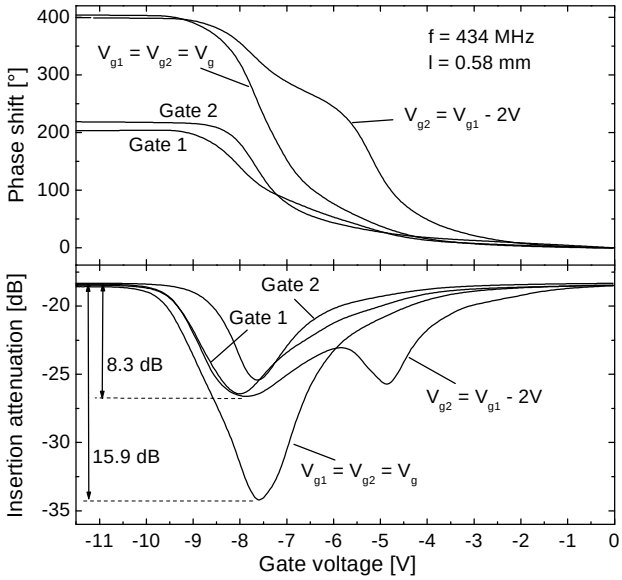

Fig. 2. Insertion attenuation and phase shift of the transmitted signal in a hybrid with two gates on top of the ELO-film according to Fig. 1 for different gate bias configurations. The quantity l denotes the length of that part of the ELO film, which is covered by gate electrodes.

This maximum attenuation can be reduced significantly, when different voltages are applied to the gates. In Fig. 2 we show a measurement, where an additional offset bias of -2 V was applied to gate 2 (see traces '$V_{g2} = V_{g1}$ - 2 V'). This results in a shift of the attenuation and phase curves of gate 2. The total phase shift is the same as for identical voltages. However, the total attenuation is much smaller when a gate voltage offset is applied, as the

overall attenuation is distributed over two different regions of the gate voltage.

A further reduction of insertion loss can be achieved by fabricating more than two gates on top of the ELO film. In Fig. 3, a hybrid with four gates is presented. The SAW characteristics of the four single gates were measured and are displayed in Fig. 3. Apart from slightly different threshold voltages, which can be explained by the fabrication process, all four gates show the expected behaviour.

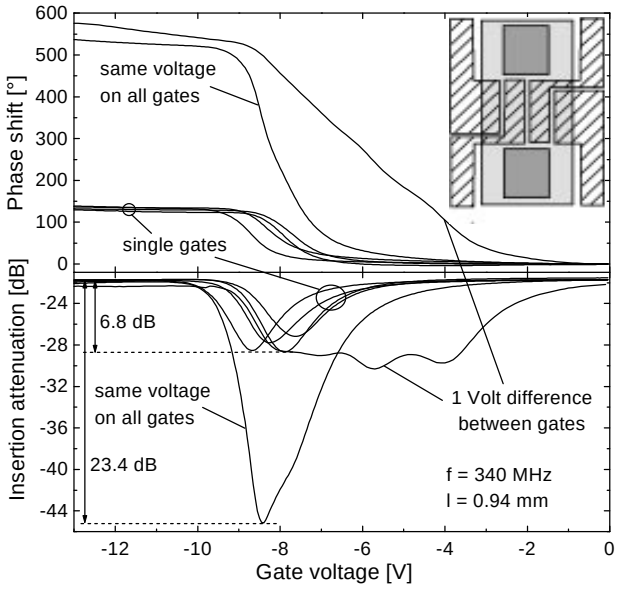

Fig. 3. Attenuation and phase shift in a device with four separated gate electrodes. The inset displays the geometry of the semiconductor structure. The color of the ELO film is light gray, the Ohmic contacts are dark gray and the gates are hatched.

When the same gate voltage is applied to all gates, the phase shifts and attenuation curves are superposed. Due to the small offsets of the single gate traces, the total attenuation is less than the sum of the maximum attenuation of the single gates. Again, the total attenuation can be distributed across a wider gate voltage range by applying different gate voltages. Here, gate bias offsets of 1 V, 2 V and 3 V were applied to the respective gate. This reduced the total electronical attenuation by 15 dB, from -23.4 dB to -8.4 . In this multiple gate device the phase shift is very close to a linear function of the gate voltage. This is very useful for most applications, where a simple linear relation between voltage and phase shift is desired. If a larger voltage offset is applied between the gates, the overall attenuation could be further minimized to a value of -6.8 dB, but this would cause steps in the phase shift curve and therefore would reduce the linearity of the phase shift.

Comparing the devices with two and four gates, it is evident that the maximum electronic attenuation in the four gate geometry is smaller than with only two gates. In addition, the phase shift as a function of gate voltage is more linear in the four gate device. On the other hand, it is more complicated to apply four different gate voltages. This could be managed with an on chip resistive voltage divider circuit or a distributed gate capacitance, which yields similar results as a constant voltage shift between the gates.

4. Continuous Potential Gradient

When the number of gate electrodes is increased, the potential drop between the electrodes becomes smaller. For a very large number, the channel potential becomes a continuous, linear function of the position in the channel. As the electron system produces significant attenuation only in the region where $\sigma = \sigma_m$, only a small area of the ELO film would contribute to the overall attenuation. Therefore we would expect a large reduction of attenuation in a geometry with a linear potential function in the channel along the SAW propagation path.

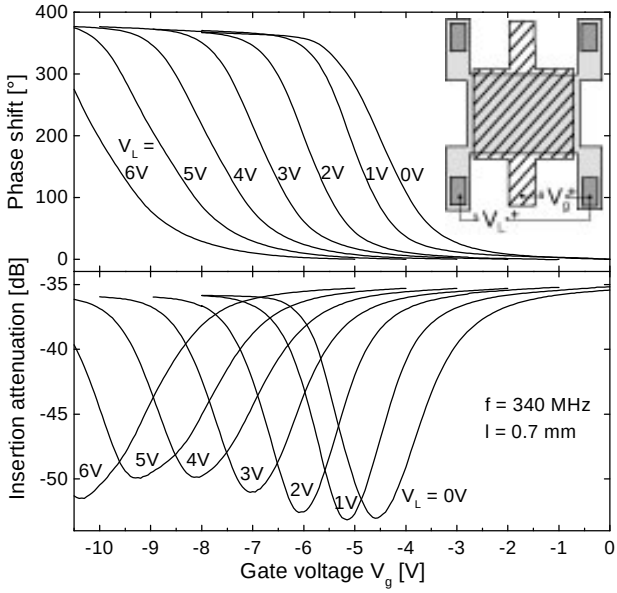

Fig. 4. SAW transmission and phase shift as a function of gate voltage with an longitudinal voltage V_L.

A potential gradient in the channel can be realized by producing a longitudinal voltage drop along the 2DES in the direction of SAW propagation, as displayed in the inset of Fig. 4. The resulting attenuation and phase shift are also shown in Fig. 4. In this setup, V_L is negative at

the left Ohmic contact in the figure, which means that the potential difference between gate and 2DES on the left hand side of the gate is V_g - V_L. Increasing the longitudinal voltage V_L thus needs also an increase of V_g in order to deplete the electron system. Therefore the maximum of attenuation shifts to larger magnitude of V_g, as can be seen in Fig. 4. When V_L is increased, the SAW transmission is reduced, reaching its minimum at about V_L = 4 V. For larger longitudinal voltage, the attenuation increases again. This can be explained with the pinch-off behavior of the semiconductor structure: for large V_L and large V_g, the right hand side of the gate is already depleted, the conductivity is very low and therefore the major part of the voltage drop of V_L occurs in this region. This prohibits a linear potential gradient in the channel and therefore a homogeneous distribution of the maximum attenuation across the total range of gate bias. This non-linear potential gradient also accounts for the relatively small reduction of the attenuation at V_g = -4 V.

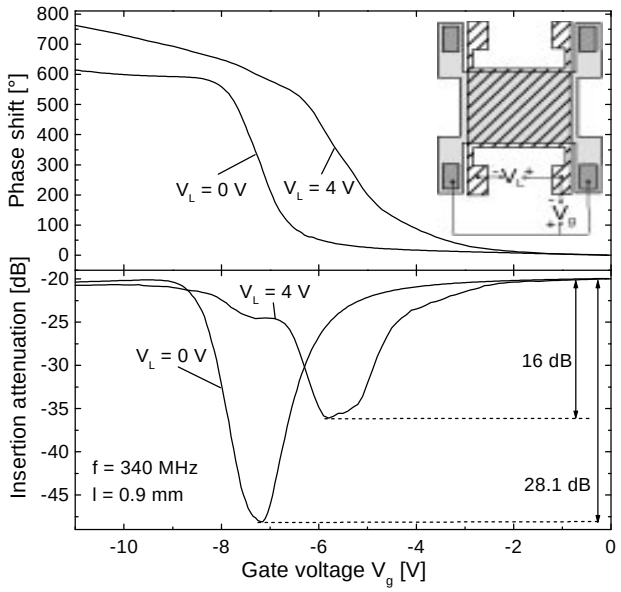

Fig. 5. Phase shift and corresponding insertion attenuation in a device with resistive (Ohmic) gate electrode. A longitudinal voltage V_L results in enhancement of SAW transmission.

A linear potential gradient can be achieved when the longitudinal voltage is applied across a resistive gate on top of the ELO film. We realized this structure with a thin Ni/Cr gate electrode (thickness 5 nm). In Fig. 5 we show the device geometry and the measured insertion loss and phase shift. If a longitudinal voltage V_L is applied, the maximum of SAW attenuation caused by the 2DES is strongly reduced. The design of a semiconductor structure with a sharper pinch-off characteristic would lead to even better results. In this first simple device, a larger voltage drop across the gate electrode leads to high currents in the gate. However, the power consumption of the gate could be strongly reduced by employing a meander-shaped gate electrode with a much larger total resistance.

5. CONCLUSIONS

The voltage controlled sheet conductivity of a semiconductor film on a $LiNbO_3$ SAW device can be employed for tuning the SAW velocity. However, at a certain conductivity σ_m, energy is dissipated by the electron system, reducing device performance at the corresponding gate bias. We demonstrate new device geometries which enhance SAW transmission significantly by a spatially inhomogenous conductivity distribution. Multiple gate structures distribute the SAW attenuation onto a wide range of gate bias and therefore reduce the maximum of attenuation presently from -23.4 dB to -8.4 dB. Due to the field effect these devices are nearly free of power consumption. Alternatively, a linear potential gradient along the gate electrode can be employed for the distribution of attenuation.

These strongly improved SAW transmission parameters allow for various SAW device applications, e.g. voltage controlled SAW oscillators, variable delay lines and SAW voltage sensors.

6. ACKNOWLEDGMENT

The authors would like to thank S. Manus, T. Ostertag and S. Berek for technical assistance. They gratefully acknowledge fruitful discussions with J. P. Kotthaus, C. C. W. Ruppel, A. Haubrich and S. Böhm. Financial support has also been provided by the German Israeli Foundation.

7. REFERENCES

1 M. Rotter, C. Rocke, S. Böhm, A. Lorke, A. Wixforth, W. Ruile and L. Korte, *Appl. Phys. Lett.* 70, 2097 (1997)
2 M. Rotter, A. Wixforth, J. P. Kotthaus, W. Ruile, D. Bernklau, H. Riechert, *Proc. IEEE Ultrasonics Symp*., Vol. I, 201 (1997)
3 E. Yablonovitch, D. M. Hwang, T. J. Gmitter, L. T. Florez and J. P. Harbison, *Appl. Phys. Lett.* 56, 2419 (1990)
4 K. Hohkawa, H. Suzuki, Q. S. Huang, and S. Noge, *Proc. IEEE Ultrasonics Symp*., 401(1995)
5 K. A. Ingebrigtsen, *J. Appl. Phys. 41*, 454 (1970)
6 A. Wixforth, J. P. Kotthaus, G. Weimann, *Phys. Rev.* B40, 7874 (1989)
7 M. Rotter, W. Ruile, A. Wixforth, J. P. Kotthaus, to be published in *IEEE Trans. Ultrason. Ferroel. Freq. Contr.*